Motion During Acquisition is Associated With fMRI Brain Entropy

Clarisse F. de Vries, Roger T. Staff, Gordon D. Waiter, Moses O. Sokunbi, Anca L. Sandu, and Alison D. Murray

***Abstract*—Measures of fMRI brain entropy have been used to investigate age and disease related neural changes. However, it is unclear if movement in the scanner is associated with brain entropy after geometric correction for movement. As age and disease can affect motor control, quantifying and correcting for the influence of movement will avoid false findings. This paper examines the influence of head motion on fMRI brain entropy. Resting-state and task-based fMRI data from 281 individuals born in Aberdeen between 1950 and 1956 were analyzed. The images were realigned, followed by nuisance regression of the head motion parameters. The images were either high-pass filtered (0.008 Hz) or band-pass (0.008–0.1 Hz) filtered in order to compare the two methods; fuzzy approximate entropy and fuzzy sample entropy were calculated for every voxel. Motion was quantified as the mean displacement and mean rotation in three dimensions. Greater mean motion was correlated with decreased entropy for all four methods of calculating entropy. Different movement characteristics produce different patterns of associations, which appear to be artefact. However, across all motion metrics, entropy calculation methods, and scan conditions, a number of regions consistently show a significant negative association: the right cerebellar crus, left precentral gyrus (primary motor cortex), the left postcentral gyrus (primary somatosensory cortex), and the opercular part of the left inferior frontal gyrus. The robustness of our findings at these locations suggests that decreased entropy in specific brain regions may be a marker for decreased motor control.**

***Index Terms*—Fuzzy approximate entropy, fuzzy sample entropy, motion, resting-state fMRI, task-based fMRI.**

I. Introduction

IN THE 1980s the field of nonlinear dynamics began to be applied to the analysis of physiological systems [1], [2]. These studies found a decrease in variability, and a decrease in fractal-like patterns, with increasing age and with the presence of disease [3]–[7]. In the early 1990's, Lipsitz and Goldberger, drawing from this early work, hypothesized that complexity is characteristic of healthy physiological systems, whereas ageing and pathologically compromised systems lose complexity [8], [9]. They observed that age and disease were negatively correlated with various nonlinear measures of complexity.

Further work supported the hypothesis that a decrease in complexity correlates with increasing age and the incidence of disease [10]–[13]. Complexity/variability measures have also been applied to the analysis of fMRI images. It has been found that fMRI brain variability measures increase with cognitive ability [14], [15] and decrease with age [15]–[17]. Furthermore, brain variability in Alzheimer's disease patients was found to be reduced relative to controls and those with mild cognitive impairment [18].

If such measures are to be truly useful in either a clinical or research setting, estimating and accounting for potential confounders is important. Movement during acquisition is particularly important in the investigation of ageing, as motor control deficits, such as gait and balance disorders, increase with age [19] and become more prevalent with the occurrence of dementia [20]. Furthermore, previous work has shown that head motion influences measures of functional connectivity [21], structural connectivity [22] and brain anatomy [23]. As a result, motion artefacts could give rise to false positive results or confound measured associations.

Here, we examine the influence of head motion on entropy using two different entropy algorithms (fuzzy approximate entropy or fApEn, and fuzzy sample entropy or fSampEn) and two types of frequency filtering (band-pass/high-pass), in order to assess the sensitivity of each approach to motion. fApEn and fSampEn are modified versions of the approximate entropy algorithm (ApEn), which Pincus developed in 1991 specifically to deal with noisy and short signals [24]. ApEn and its alterations are often used in the analysis of biological systems, where limited acquisition time (restricting the number of data points) and measurement noise are points of concern. Band-pass and high-pass filters are often used in fMRI (entropy) analyses to reduce noise [17], [25].

The aim of this study is to determine the association between participants' brain entropy measured using resting-state and task-based fMRI data and their head motion during acquisition, after standard motion correction techniques are performed. We hypothesize that increased motion during acquisition is

Manuscript received October 15, 2018; revised January 21, 2019 and March 4, 2019; accepted March 19, 2019. Date of publication April 1, 2019; date of current version February 6, 2020. This work was supported in part by the University of Aberdeen Development Trust (DT OL1134) and in part by the Wellcome Trust (104036/Z/14/Z). *(Corresponding author: Roger T. Staff.)*

C. F. de Vries, G. D. Waiter, A. L. Sandu, and A. D. Murray are with the Aberdeen Biomedical Imaging Centre, University of Aberdeen, Aberdeen AB24 3FX, U.K. (e-mail: r02cfd15@abdn.ac.uk; g.waiter@abdn.ac.uk; anca.sandu-giuraniuc@abdn.ac.uk; a.d.murray@abdn.ac.uk).

R. T. Staff is with the Department of Imaging Physics, NHS Grampian, Aberdeen AB15 6RE, U.K. (e-mail: r.staff@nhs.net).

M. O. Sokunbi is with the Faculty of Health and Life Sciences, De Montfrot University, Leicester LE1 9BH, U.K. (e-mail: moses.sokunbi@dmu.ac.uk).

Digital Object Identifier 10.1109/JBHI.2019.2907189

TABLE I
DEMOGRAPHICS AND ENTROPY MEASURES OF SAMPLE

	Resting-state		*Fearful*		*Reward*	
	Values	min-max	Values	min-max	Values	min-max
Number of participants	281	-	280	-	279	-
Sex-Number Male	127, 45.2%	-	128, 45.7%	-	128, 45.9%	-
Whole brain entropy						
fApEn + hpf	0.986 (0.001)	0.908-1.006	0.898 (0.001)	0.845-0.918	0.989 (0.001)	0.936-1.004
fApEn + bpf	0.589 (0.001)	0.537-0.619	0.555 (0.001)	0.501-0.580	0.588 (0.001)	0.551-0.615
fSampEn + hpf	1.594 (0.004)	1.307-1.691	1.602 (0.001)	1.285-1.690	1.599 (0.001)	1.350-1.692
fSampEn + bpf	0.698 (0.002)	0.579-0.762	0.694 (0.004)	0.584-0.749	0.704 (0.004)	0.623-0.774

Numbers in brackets indicate standard error of mean. fApEn, fuzzy approximate entropy; fSampEn, fuzzy sample entropy; hpf, high-pass filter; bpf, band-pass filter.

associated with decreased estimates of entropy. If different components of motion (translation and rotation in 3 directions) produce different associations, these associations can be interpreted as artefact. However, if a consistent relationship between entropy and motion is found, brain entropy may be associated with motor function and motor control. A relationship consistent across scan conditions suggests that the associations observed are not caused by the particular head movements shown during one type of scan. Furthermore, because participants are asked to stay as still as possible in the scanner in order to minimize the effect of movement on image quality, their involuntary motion could be associated with motor control. Therefore, a consistent relationship across motion components would suggest an association between entropy and motor function. In the first instance we use a parametric mapping to test for associations. In addition, we use the average entropy in 95 grey matter regions to examine the overlapping nature of these findings.

II. METHODS

A. Sample

The analyses were performed on a subset of the Aberdeen Children of the 1950s (ACONF) dataset (see Table I) [26]. Participants were born between 1950 and 1956 in Aberdeen. The Stratifying Resilience and Depression Longitudinally (STRADL) study, a collaboration between researchers in Edinburgh and Aberdeen, was funded by the Wellcome Trust in 2014 to study depression [27]. STRADL received ethical approval from the NHS Tayside committee on research ethics (14/SS/0039). As part of STRADL, a subset of individuals in the ACONF dataset were recruited for brain imaging. Participants were imaged using a 3 T MR system (Philips Achieva TX-series). MRI included a T1-weighted volumetric scan (repetition time (TR)/echo time (TE) = 8.3/3.8 ms; matrix = 240 × 240; n slices = 160; thickness = 1 mm) and functional imaging (TR = 1560 ms, TE = 26 ms, 32 transverse slices, matrix = 64 × 64, pixel size = 3.39 × 3.39 mm^2, slice thickness = 4.5 mm). fMRI consisted of a resting-state scan (195 volumes) and two task-based scans, "Fearful" (154 volumes) and "Reward" (573 volumes). For Fearful, participants were shown fearful and neutral faces using a blocked design. For Reward, participants completed an instrumental reward task. The images of the first participants scanned (N = 281) were used. The age of the participants at time of MRI ranged from 59 to 65.

B. Algorithms

Pincus proposed a family of statistics called approximate entropy (ApEn) to quantify and analyse the complexity of physiological data [24]. ApEn examines the complexity of a signal by determining its irregularity. The ApEn algorithm divides the signal into blocks (or vectors) of length *m*. It then determines the similarity of each vector X_i^m with itself and every other vector; vectors are either classified as similar or non-similar. This classification depends on a pre-specified tolerance value *r*, defined as a constant multiplied by the standard deviation of the signal. The discontinuous Heaviside step function Θ assigns a value of 1 when the distance between the vectors is smaller than the tolerance *r* (i.e., similar), and a value of 0 when the distance is greater than *r* (i.e., non-similar). For each vector, the logarithm of the average value of these classifications is computed. Then, these logarithms for each vector are averaged, yielding $\phi^m(r)$. This process is repeated for $m+1$, resulting in $\phi^{m+1}(r)$. ApEn is then calculated as the difference between $\phi^m(r)$ and $\phi^{m+1}(r)$.

Formally, for a signal of length *N* ApEn is defined as:

$$ApEn(m,r,N) = \phi^m(r) - \phi^{m+1}(r) \tag{1}$$

where

$$\phi^m(r) = [N-m+1]^{-1} \sum_{i=1}^{N-m+1} \ln C_i^m(r) \tag{2}$$

and

$$C_i^m(r) = [N-m+1]^{-1} \sum_{j=1}^{N-m+1} \Theta\left(d_{ij}^m - r\right) \tag{3}$$

d_{ij}^m is the distance between two m-dimensional vectors X_i^m and X_j^m:

$$d_{ij}^m = d[X_i^m, X_j^m] = \max_{k\in(0,m-1)} |u(i+k) - u(j+k)| \tag{4}$$

Vector sequences are formed as follows:

$$X_i^m = \{u(i), u(i+1), \ldots, u(i+m-1)\} \tag{5}$$

with *i* and *j* ranging from 1 to $N-m+1$.

Θ is the discontinuous Heaviside step function, defined as:

$$\Theta(z) = \begin{cases} 1 \text{ if } z \le 0 \\ 0 \text{ if } z > 0 \end{cases} \tag{6}$$

An alteration to ApEn is sample entropy (SampEn) [28]. For ApEn every vector is always matched with itself, which avoids taking the logarithm of zero in the case that no matches occur ($C_i^m = 0$ would result in ln(0), which is not defined mathematically). However, for short datasets this self-matching disproportionally affects the ApEn value by artificially increasing the similarity, thus decreasing the entropy value. Thus, ApEn is dependent on the length of the time series. Unlike ApEn, SampEn does not count so-called self-matches. The logarithm is taken at the last step, avoiding ln(0) if $C_i^m = 0$. Furthermore, only the first $N - m$ vectors of length m are considered for both m and $m + 1$, ensuring that, for i between 1 and $N - m$, X_i^m and X_i^{m+1} are defined.

For a signal of length N SampEn is defined as follows:

$$SampEn\,(m, r, N) = -\ln\left[\frac{U^{m+1}\,(r)}{U^{m}\,(r)}\right] \tag{7}$$

where

$$U^m\,(r) = [N-m]^{-1}\sum_{i=1}^{N-m} C_i^m\,(r) \tag{8}$$

and

$$C_i^m\,(r) = [N-m-1]^{-1}\sum_{j=1}^{N-m} \Theta\left(d_{ij}^m - r\right) \tag{9}$$

d_{ij}^m is the distance between two m-dimensional vectors X_i^m and X_j^m:

$$d_{ij}^m = d[X_i^m, X_j^m] = \max_{k\in(0,m-1)} |u(i+k) - u(j+k)| \tag{10}$$

Vector sequences are formed as follows:

$$X_i^m = \{u\,(i), u\,(i+1), \ldots, u\,(i+m-1)\} \tag{11}$$

$$X_i^{m+1} = \{u\,(i), u\,(i+1), \ldots, u\,(i+m)\} \tag{12}$$

with i ranging from 1 to $N - m$, and j ranging from 1 to $N - m$ with $j \neq i$.

Zadeh's concept of fuzzy sets [29] was proposed as an improvement on the ApEn and SampEn algorithms [30]–[32]. Zadeh argued that the real physical world often lacks unambiguous and clear boundaries between classes, and that in certain cases it could be more appropriate to consider degrees of membership, versus simply inclusion or exclusion. For 'fuzzy approximate entropy' (fApEn) and 'fuzzy sample entropy' (fSampEn), instead of classifying the vectors as either similar or non-similar, the Heaviside step function is replaced by a continuous function which decides their degree of similarity. Fuzzy entropy showed increased monotonicity, relative consistency, and robustness to noise. Furthermore, fuzzy entropy offers an improved assessment of signal complexity and a decreased dependence on data length. Here, we use the fuzzy membership function suggested by Sokunbi *et al.* [17]:

$$\mu\,(x) = \begin{cases} 0.5\left(2 - x^2\right) & \text{if } 0 \le x \le 1 \\ 0.5(2-x)^2 & \text{if } 1 < x \le 2 \end{cases} \tag{13}$$

with x defined as distance/r.

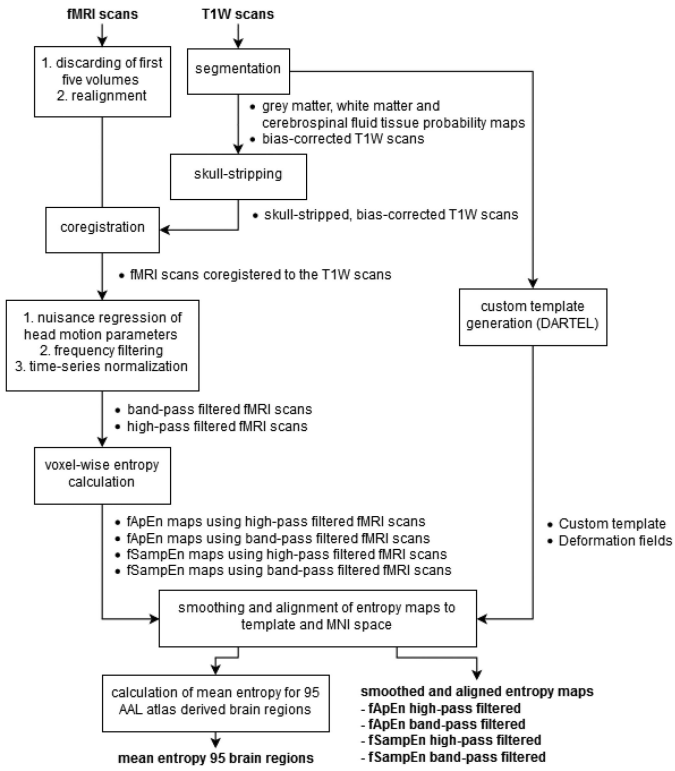

Fig. 1. Image processing pipeline.

C. Image Pre-Processing and Generation of Entropy Maps

Fig. 1 gives an overview of the resting-state and task-based fMRI processing pipeline. The reward scan was truncated from 573 to the first 195 volumes acquired to improve its comparability with the resting-state and fearful scans. The first five volumes of the fMRI scans were discarded to allow for the magnetization to reach its steady state. Using SPM12, the fMRI brain scans were realigned by a rigid-body spatial transformation, followed by nuisance regression of the six SPM12 estimated head motion parameters (rotation and displacement in three dimensions). Global signal regression was not performed. Global signal regression is controversial [33], and its influence on brain entropy analyses is unclear.

The images were either high-pass filtered (0.008 Hz) or band-pass filtered (0.008 Hz–0.1 Hz) in order to compare the two methods. Because low-pass filtering increases the autocorrelation of a given time-series, it is expected that band-pass filtering (high-pass + low-pass filtering) would result in lower values of entropy (a measure of variability) than high-pass filtering alone. The time series at every voxel was then rescaled to a standard deviation of 1. This allowed the use of one r-value (constant × standard deviation of signal) for all voxels of the brain. fApEn and fSampEn were calculated for every voxel, generating 12 3D brain entropy maps per participant (4 methods applied to 3 types of scans). Parameter values were chosen as $m = 2$, and $r = 0.25$. These values have been previously used in an fApEn analysis of resting-state fMRI signal complexity [17]. For each participant, and from each of the four entropy maps, whole brain entropy

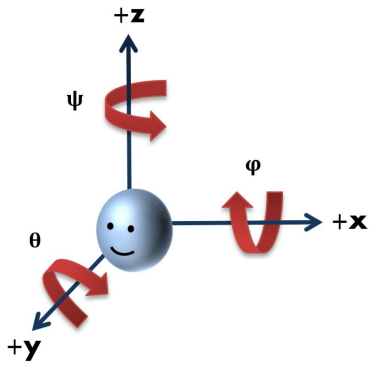

Fig. 2. Head position relative to x, y and z axes and φ, θ and ψ rotations.

was calculated by taking the mean of the entropy in all brain voxels.

In order to align the entropy maps with each other to examine regional differences between groups, the following process was followed. The structural T1-weighted MRI scans were segmented, which generated grey matter, white matter and cerebrospinal fluid probability maps. The fMRI scans were coregistered with the skull-stripped and bias-corrected T1-weighted scans. Skull-stripping and bias-correcting (which corrects for intensity inhomogeneities) the T1-weighted scans allows for a better coregistration between functional and anatomical scans. Employing the segmented T1-weighted scans, DARTEL was used to create a custom brain template in MNI space. The entropy maps were then smoothed with an 8 mm kernel and normalised to the template. In addition, using the smoothed and aligned entropy maps, the average entropy for 95 grey matter brain regions, derived from the Automated Anatomical Labeling (AAL) atlas [34], was calculated for each participant.

D. Motion Metrics

Measures of motion were quantified using the six head motion parameters that are estimated by the rigid body spatial transformation utilized in the process of fMRI realignment. The x, y and z directions and φ, θ and ψ rotations relative to the person's head are illustrated in Fig. 2. For each direction x (left/right), y (forward/backward) and z (up/down), the mean of the absolute value of the between-frame x, y and z translation was calculated, resulting in the measures mean x-displacement, y-displacement, and z-displacement. φ (pitch), θ (roll) and ψ (yaw) are the rotations around the x, y and z-axes, respectively. The mean of the absolute value of the between-frame φ, θ and ψ rotation was used to quantify participants' global head rotation. This resulted in the measures mean φ-rotation, θ-rotation and ψ-rotation. To correct for positive skew, the above described motion metrics were log-transformed.

Factor analysis was used to extract one main component from the six log-transformed measures of head motion (mean x, y and z displacement, and mean φ, θ and ψ rotation), in order to examine the relationship between the shared variance of these measures and brain entropy. For resting-state, the main component describes 64.2% of the total variance (component loadings: mean x-displacement .721, mean y-displacement .758, mean z-displacement .824, mean φ-rotation .812, mean θ-rotation .856, mean ψ-rotation .827). For fearful, the main component describes 60.7% of the total variance (component loadings: mean x-displacement .732, mean y-displacement .691, mean z-displacement .792, mean φ-rotation .846, mean θ-rotation .868, mean ψ-rotation .728). For reward, the main component describes 63.2% of the total variance (component loadings: mean x-displacement .727, mean y-displacement .709, mean z-displacement .827, mean φ-rotation .826, mean θ-rotation .864, mean ψ-rotation .805).

E. Statistical Analysis

First, the relationship between resting-state brain entropy and the seven motion metrics was assessed, for each of the four methods of calculating entropy (type of entropy algorithm, fApEn or fSampEn, and type of frequency filtering, band-pass or high-pass). Global associations were examined using Pearson's correlation (SPSS version 24). Regional associations were examined in two ways. Motion and entropy associations were assessed for every voxel with SPM12 (version 6906), using linear regression. Family-wise error (FWE) correction ($p_{FWE} < .05$) was utilized to correct for multiple comparisons. In addition, the relationship between the mean entropy in the 95 brain regions and the seven motion metrics was assessed, using Pearson's correlation with false discovery rate (FDR) correction ($p_{FDR} < .05$). Second, the relationship between the regional task-based entropy measures and the composite motion metric was assessed for every voxel ($p_{FWE} < .05$). All renders were generated with the SPM plug-in BRANT.

III. Results

The whole brain entropy and motion measures for the sample are shown in Table I and Fig. 3, respectively. As expected, the fSampEn measures (which avoid self-matches) were higher than the fApEn measures. And as predicted, band-pass filtering decreased the entropy value relative to high-pass filtering by increasing the autocorrelation of the fMRI time-series. Participants' mean displacement was greatest in the z-direction, and smallest in the y-direction. Participants' mean rotation was greatest in the φ-direction and smallest in the ψ-direction. Pairwise comparisons show that each whole brain entropy and motion measure was significantly correlated with itself across the three scans ($p < .001$). The Pearson's correlation coefficient R ranged from .319 to .673 for the entropy measures, and from .691 to .933 for the motion measures.

A. Resting-State Analysis

Table II shows that all motion metrics, apart from mean x-displacement, were negatively correlated with the four measures of resting-state global entropy ($p < .05$), i.e., an increase in motion was correlated with a decrease in entropy.

The voxel-wise SPM correlation between the entropy maps and the movement estimates is shown in Fig. 4. The results for each movement dimension and the composite metric, for the two

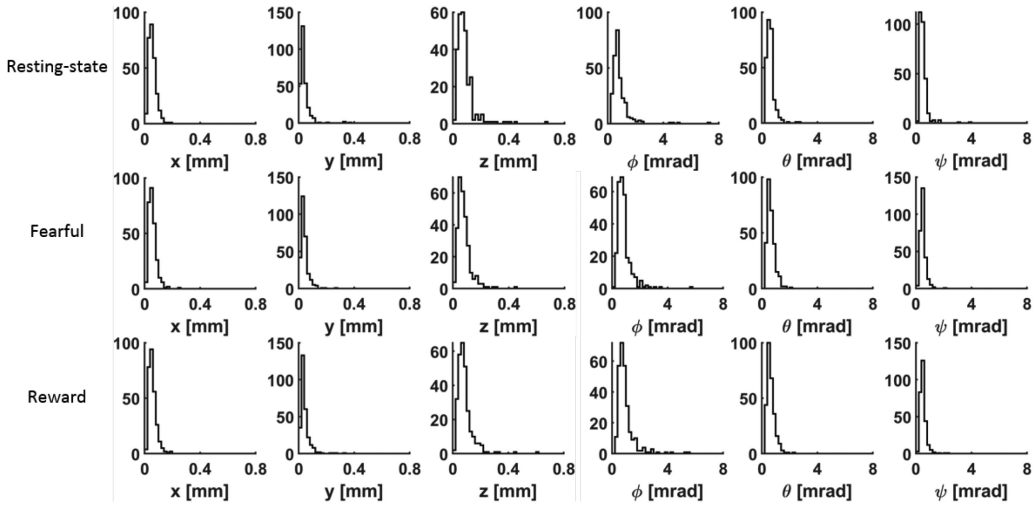

Fig. 3. Histograms of the six mean motion measures (x, y, and z displacement, and φ, θ and ψ rotation) for the three scans.

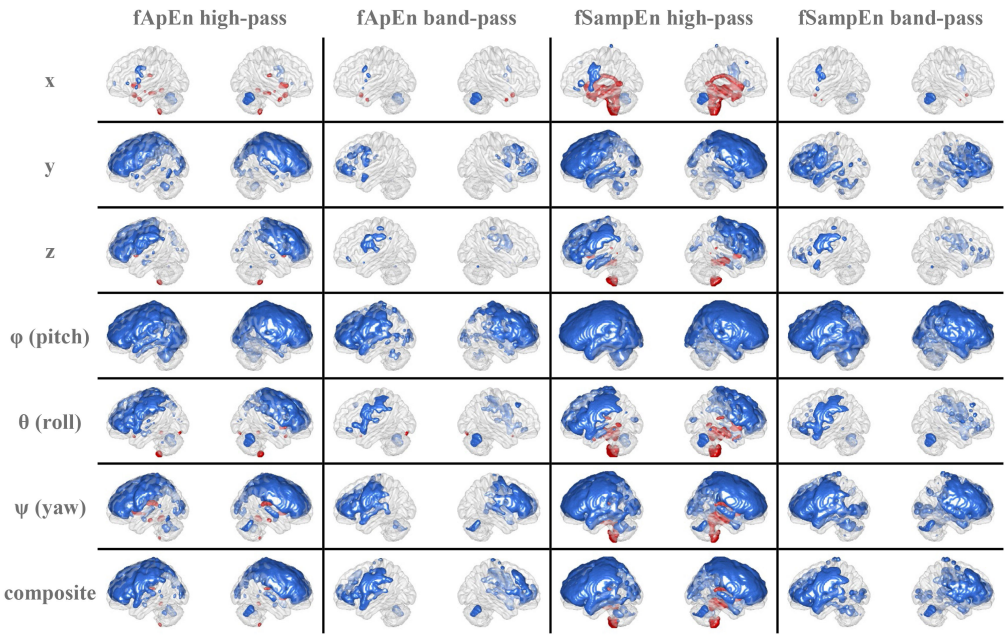

Fig. 4. Motion was significantly associated with resting-state entropy, for all entropy and motion measures. Positive associations are shown in red, negative associations in blue.

methods of frequency filtering and the two methods of entropy calculation were calculated. On each occasion there was a negative correlation between movement and entropy at a number of locations. On a number of occasions, a positive correlation was seen at the brainstem, right olfactory cortex, right thalamus, and cerebellar vermis. Regarding sensitivity, band-pass filtering and the fApEn algorithm produced less extensive significant associations between movement and entropy than high-pass filtering and fSampEn. As expected, the individual movement dimensions produced different patterns of significance, with the rotation parameters producing more significant locations than the displacement parameters. However, certain areas show a negative association with all movement dimensions. Visually, it appears that entropy in the right cerebellum and left precentral gyrus is consistently associated with motion. Additionally performing nuisance regression of white matter/cerebrospinal fluid signals and correcting for age and sex did not significantly change these results. Furthermore, repeating the analyses with $r = 0.2$ and $r = 0.3$ again revealed a robust association in the above identified regions, and similar associations as seen before. Of note, however, for fApEn combined with the high-pass filter, significantly less widespread associations were seen for $r = 0.2$.

Further investigating the association between regional entropy and motion, we examined the correlation between the mean entropy in each of the 95 AAL atlas derived brain regions and the six movement components. As with the voxel-wise SPM findings, different dimensions of motion show

TABLE II
PEARSON'S CORRELATIONS BETWEEN MEAN BRAIN RESTING-STATE ENTROPY AND MOTION MEASURES

	fApEn + hpf		*fApEn + bpf*		*fSampEn + hpf*		*fSampEn + bpf*	
	R	*p*	*R*	*p*	*R*	*p*	*R*	*p*
Mean x	-.098	.100	-.040	.507	-.082	.171	-.073	.220
Mean y	-.333	<.001	-.223	<.001	-.311	<.001	-.278	<.001
Mean z	-.249	<.001	-.138	.020	-.216	<.001	-.172	.004
Mean φ	-.432	<.001	-.320	<.001	-.440	<.001	-.389	<.001
Mean θ	-.235	<.001	-.118	.048	-.197	.001	-.170	.004
Mean ψ	-.300	<.001	-.247	<.001	-.312	<.001	-.325	<.001
Composite	-.337	<.001	-.220	<.001	-.315	<.001	-.285	<.001

The mean movement components (x, y, z, ϕ, θ and φ) were log-transformed prior to statistical analysis. fApEn, fuzzy approximate entropy; fSampEn, fuzzy sample entropy; hpf, high-pass filter; bpf, band-pass filter.

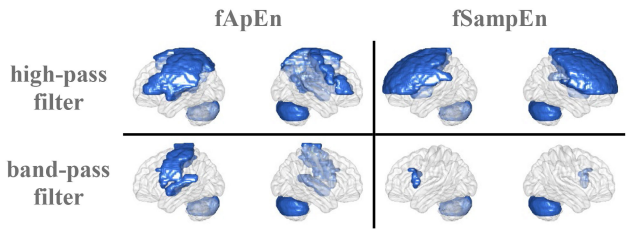

Fig. 5. Significant negative correlations between resting-state entropy and motion, common to all motion components.

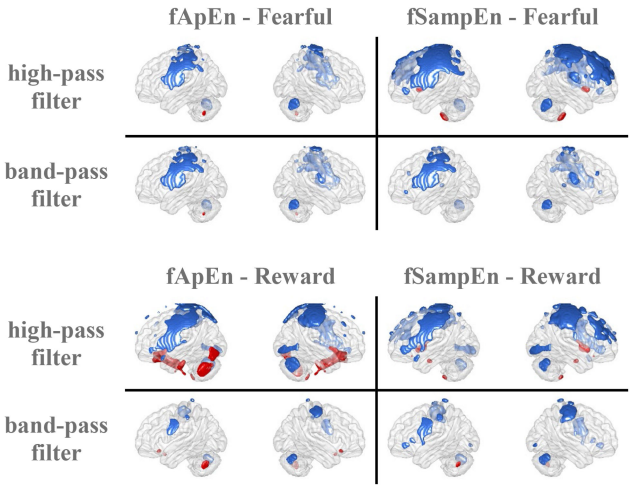

Fig. 6. Significant correlations between task-based entropy ("Fearful" and "Reward") and the composite motion metric. Red indicates positive associations, blue negative associations.

different patterns of associations. However, the results again indicate that a number of locations consistently show a negative association between entropy and motion, regardless of the movement component tested. The significant brain areas common to all movement components (x, y, z, φ, θ and ψ) are shown in Fig. 5.

For all four methods of calculating entropy, the right cerebellar crus and opercular part of the left inferior frontal gyrus are negatively associated with all movement components. For three of the four methods, the left postcentral gyrus and left precentral gyrus are negatively associated with all movement components.

B. Task-Based Analysis

As an additional analysis, we investigated the relationship between the composite motion metric and task-based entropy. Fig. 6 shows the significant brain regions for Fearful and Reward. Compared to resting-state, less widespread associations are seen for both task-based analyses. Furthermore, the found regions again include the right cerebellar crus, opercular part of the left inferior frontal gyrus, left postcentral gyrus, and left precentral gyrus.

IV. DISCUSSION

Head motion during acquisition is associated with measures of brain entropy after the application of standard motion correction techniques. Different dimensions of motion show different patterns of associations in the entropy brain maps, which could predominantly be described as artefact. However, a considerable amount of overlap could be identified, across scans and motion/entropy metrics. A consistent negative association between entropy and motion was found in the right cerebellar crus and left precentral gyrus (primary motor cortex), two regions associated with movement. Other regions identified are the opercular part of the left inferior frontal gyrus and the left postcentral gyrus (primary somatosensory cortex). The primary somatosensory cortex is involved in proprioception, which plays a role in motor control [35], [36]. As the commonality between the motion measures is an (in)ability to stay still in the scanner, lower entropy in these regions may indicate reduced motor control, rather than motion artefacts.

Previous studies show both positive and negative associations between head motion and BOLD signals [37], [38], brain structure [39], and various other derivative brain measures [22], [40], [41]. Furthermore, the directions of these associations are location-dependent. These non-uniform relationships can be partially explained by the unequal distribution of motion across voxels in the brain [37], [38], with the largest movement found in the prefrontal cortex. Although not further explored here, this spatial heterogeneity of the head motion may be a confounding factor of the reported spatial distribution of the entropy-motion association. It has also been suggested that associations between BOLD and motion which withstood stringent motion correction (observed in the motor and motor-sensitive visual areas) may reflect motion-related neural activity [38]. We similarly show non-uniform positive and negative associations between motion and entropy. In addition, entropy/complexity in specific brain regions may be associated with motor processes and function.

We show less widespread associations between motion and entropy for the task-based analyses than for resting-state. Relative to rest, participants exhibit more head motion when performing a motor-task [42], but less during cognitive tasks [43]. Here, both fMRI tasks require motor-responses and some degree of cognitive involvement.

These results indicate that it is prudent to consider the influence of head motion on entropy, and draw into question previous results that have demonstrated associations between an external measure, such as disease state, and entropy in a resting-state

fMRI context. For example, individuals with Alzheimer's disease and mild cognitive impairment show increased head motion in the scanner relative to controls [44]. Overlooking the possible influence of motion may lead to observing movement artefacts, rather than mechanisms underlying disease processes. It should be examined whether the covariates of interest (or groups compared) are associated with motion. If an association is found, false positive findings could occur. If no association is found, motion could be considered a confounder. The significance of any found association between the covariate of interest and entropy is then possibly an underestimate due to the variance added by motion.

One approach to correcting for head motion is to include the six global measures of motion as covariates in the statistical models. However, due to the reduction in degrees of freedom, a large amount of data would be needed. Furthermore, if entropy in certain regions is indeed associated with motor control, a too stringent motion correction could result in false negative findings. Adjusting for some summary variable may provide a practical solution, although the merits of different summary variables are unclear. An alternative approach would be to examine the variance in the variable of interest that is not associated with movement. This could be done by regressing out the motion component from the covariate of interest prior to investigating the association with entropy. Additional motion correction steps, such as spike regression, scrubbing, and a higher-parameter confound regression model [37], could also be employed.

When movement is a concern, band-pass filtering might be preferred over high-pass filtering, and fApEn over fSampEn. Band-pass filtering reduced the influence of motion relative to high-pass filtering. Band-pass filtering removed the high frequencies from the fMRI time-series ($>$0.1 Hz), which contain movement-related noise [37], in addition to the low frequencies ($<$0.008 Hz). Furthermore, low-pass filtering (or smoothing in the time domain) decreases measures of entropy by increasing the self-similarity of the fMRI time-series. Moreover, the fSampEn algorithm, which avoids self-matches and has greater dynamic range than fApEn, showed increased sensitivity to motion than fApEn. However, this poses a trade-off between sensitivity and specificity, with reports suggesting that there is valuable information in the frequencies above 0.1 Hz [45], [46].

The main weakness of our analysis is that we are not able to isolate a particular movement dimension independently of the other dimensions. Our data indicate that movement between frames is rarely limited to a single dimension. The six degrees of freedom and the length of the fMRI time-series (190 time points) make a classification of types of movement complex, and the motion data difficult to meaningfully reduce. This prevents us from fully characterizing the motion and the resulting associations/artefacts. Moreover, numerous methods have been employed to calculate brain entropy. For example, entropy can be calculated after the fMRI scans are normalized to MNI space, instead of before (as done here). Therefore, our work may not generalize to different brain entropy analyses. Furthermore, in past work, the entropy parameter values are often optimized for the specific measure(s) under consideration. The choice of r and m could influence the relationship between entropy and motion, and might also change the algorithms' relative sensitivity to motion. However, here we examined motion as a nuisance variable, with no separate measure to optimise for. In addition, an optimization procedure could lead to different r and m-values for the four methods of calculating entropy. Any differences found could then be attributable to the different parameter values, as opposed to the methods employed. Finally, our analysis does not definitively establish the direction of causality. For instance, individuals who move more while undergoing MRI scanning might have inherent and widespread differences in brain entropy relative to individuals who move less. Although we have not excluded this possibility, here we find that motion is consistently associated with entropy in specific brain regions known to be involved in motor function.

In summary, motion can be a concern in fMRI brain entropy analyses. Careful consideration of pre-processing methods and entropy algorithm, based on the groups compared or variable(s) of interest examined, is advised. Possibly, greater complexity in a number of brain areas, including the motor cortex, is reflective of a neural network that is involved in motor control.

Acknowledgment

The authors would like to thank the participants who contributed to this study. They would also like to thank the staff of the Aberdeen Biomedical Imaging Centre and the research team involved in the recruitment and imaging of the participants.

References

[1] A. L. Goldberger and B. J. West, "Applications of nonlinear dynamics to clinical cardiology," *Ann. New York Acad. Sci.*, vol. 504, no. 1, pp. 195–213, 1987.

[2] B. J. West and A. L. Goldberger, "Physiology in fractal dimensions," *Am. Sci.*, vol. 75, no. 4, pp. 354–365, 1987.

[3] L. A. Lipsitz, J. Mietus, G. B. Moody, and A. L. Goldberger, "Spectral characteristics of heart rate variability before and during postural tilt: Relations to aging and risk of syncope," *Circulation*, vol. 81, no. 6, pp. 1803–1810, Jun. 1990.

[4] D. Kaplan, M. Furman, S. Pincus, S. Ryan, L. Lipsitz, and A. Goldberger, "Aging and the complexity of cardiovascular dynamics," *Biophys. J.*, vol. 59, no. 4, pp. 945–949, 1991.

[5] R. E. Dustman, J. A. LaMarche, N. B. Cohn, D. E. Shearer, and J. M. Talone, "Power spectral analysis and cortical coupling of EEG for young and old normal adults," *Neurobiol. Aging*, vol. 6, no. 3, pp. 193–198, Fall 1985.

[6] S. L. Greenspan, A. Klibanski, J. W. Rowe, and D. Elahi, "Age-related alterations in pulsatile secretion of TSH: Role of dopaminergic regulation," *Am. J. Physiol.*, vol. 260, no. 3 Pt 1, pp. E486–E491, Mar. 1991.

[7] L. Mosekilde, "Age-related changes in vertebral trabecular bone architecture—Assessed by a new method," *Bone*, vol. 9, no. 4, pp. 247–250, 1988.

[8] L. A. Lipsitz and A. L. Goldberger, "Loss of complexity and aging," *JAMA*, vol. 267, no. 13, pp. 1806–1809, 1992.

[9] R. Pool, "Is it healthy to be chaotic?" *Science*, vol. 243, no. 4891, pp. 604–607, 1989.

[10] L. A. Lipsitz, "Dynamics of stability: The physiologic basis of functional health and frailty," *J. Gerontol. A, Biol. Sci. Med. Sci.*, vol. 57, no. 3, pp. B115–B125, 2002.

[11] H. M. Al-Angari and A. V. Sahakian, "Use of sample entropy approach to study heart rate variability in obstructive sleep apnea syndrome," *IEEE Trans. Biomed. Eng.*, vol. 54, no. 10, pp. 1900–1904, Oct. 2007.

[12] A. Sandu *et al.*, "Structural brain complexity and cognitive decline in late life—A longitudinal study in the Aberdeen 1936 Birth Cohort," *Neuroimage*, vol. 100, pp. 558–563, 2014.

[13] D. Mateos, R. G. Erra, R. Wennberg, and J. P. Velazquez, "Measures of entropy and complexity in altered states of consciousness," *Cogn. Neurodyn.*, vol. 12, no. 1, pp. 73–84, 2018.
[14] M. O. Sokunbi *et al.*, "Inter-individual differences in fMRI entropy measurements in old age," *IEEE Trans. Biomed. Eng.*, vol. 58, no. 11, pp. 3206–3214, Nov. 2011.
[15] A. C. Yang *et al.*, "Complexity of spontaneous BOLD activity in default mode network is correlated with cognitive function in normal male elderly: A multiscale entropy analysis," *Neurobiol. Aging*, vol. 34, no. 2, pp. 428–438, Feb. 2013.
[16] M. O. Sokunbi, "Sample entropy reveals high discriminative power between young and elderly adults in short fMRI data sets," *Front. Neuroinform.*, vol. 8, pp. 1–12, 2014.
[17] M. O. Sokunbi, G. G. Cameron, T. S. Ahearn, A. D. Murray, and R. T. Staff, "Fuzzy approximate entropy analysis of resting state fMRI signal complexity across the adult life span," *Med. Eng. Phys.*, vol. 37, no. 11, pp. 1082–1090, 2015.
[18] B. Wang *et al.*, "Decreased complexity in Alzheimer's disease: Resting-state fMRI evidence of brain entropy mapping," *Front. Aging Neurosci.*, vol. 9, pp. 1–11, 2017.
[19] J. Verghese, A. LeValley, C. B. Hall, M. J. Katz, A. F. Ambrose, and R. B. Lipton, "Epidemiology of gait disorders in community-residing older adults," *J. Am. Geriatr. Soc.*, vol. 54, no. 2, pp. 255–261, 2006.
[20] L. M. Allan, C. G. Ballard, D. J. Burn, and R. A. Kenny, "Prevalence and severity of gait disorders in Alzheimer's and Non-Alzheimer's dementias," *J. Am. Geriatr. Soc.*, vol. 53, no. 10, pp. 1681–1687, 2005.
[21] K. R. Van Dijk, M. R. Sabuncu, and R. L. Buckner, "The influence of head motion on intrinsic functional connectivity MRI," *Neuroimage*, vol. 59, no. 1, pp. 431–438, 2012.
[22] G. L. Baum *et al.*, "The impact of in-scanner head motion on structural connectivity derived from diffusion MRI," *Neuroimage*, vol. 173, pp. 275–286, 2018.
[23] A. Alexander-Bloch *et al.*, "Subtle in-scanner motion biases automated measurement of brain anatomy from in vivo MRI," *Hum. Brain Mapping*, vol. 37, no. 7, pp. 2385–2397, 2016.
[24] S. M. Pincus, "Approximate entropy as a measure of system complexity," *Proc. Nat. Acad. Sci. USA*, vol. 88, no. 6, pp. 2297–2301, Mar. 15, 1991.
[25] Y. Jia, H. Gu, and Q. Luo, "Sample entropy reveals an age-related reduction in the complexity of dynamic brain," *Sci. Rep.*, vol. 7, no. 1, 2017, Art. no. 7990.
[26] G. D. Batty *et al.*, "The Aberdeen children of the 1950s cohort study: Background, methods and follow-up information on a new resource for the study of life course and intergenerational influences on health," *Paediatr. Perinatal Epidemiol.*, vol. 18, no. 3, pp. 221–239, 2004.
[27] L. Navrady *et al.*, "Cohort profile: Stratifying resilience and depression longitudinally (STRADL): A questionnaire follow-up of Generation Scotland: Scottish Family Health Study (GS: SFHS)," *Int. J. Epidemiol.*, vol. 47, no. 1, pp. 13–14, 2017.
[28] J. S. Richman and J. R. Moorman, "Physiological time-series analysis using approximate entropy and sample entropy," *Am. J. Physiol., Heart Circul. Physiol.*, vol. 278, no. 6, pp. H2039–H2049, 2000.
[29] L. A. Zadeh, "Fuzzy sets," *Inf. Control*, vol. 8, no. 3, pp. 338–353, 1965.
[30] W. Chen, J. Zhuang, W. Yu, and Z. Wang, "Measuring complexity using fuzzyen, apen, and sampen," *Med. Eng. Phys.*, vol. 31, no. 1, pp. 61–68, 2009.
[31] H. Xie, J. Guo, and Y. Zheng, "Fuzzy approximate entropy analysis of chaotic and natural complex systems: Detecting muscle fatigue using electromyography signals," *Ann. Biomed. Eng.*, vol. 38, no. 4, pp. 1483–1496, 2010.
[32] G. Xiong, L. Zhang, H. Liu, H. Zou, and W. Guo, "A comparative study on ApEn, SampEn and their fuzzy counterparts in a multiscale framework for feature extraction," *J. Zhejiang Univ. Sci. A*, vol. 11, no. 4, pp. 270–279, 2010.
[33] K. Murphy and M. D. Fox, "Towards a consensus regarding global signal regression for resting state functional connectivity MRI," *Neuroimage*, vol. 154, pp. 169–173, 2017.
[34] N. Tzourio-Mazoyer *et al.*, "Automated anatomical labeling of activations in SPM using a macroscopic anatomical parcellation of the MNI MRI single-subject brain," *Neuroimage*, vol. 15, no. 1, pp. 273–289, 2002.
[35] B. L. Riemann and S. M. Lephart, "The sensorimotor system, Part I: The physiologic basis of functional joint stability," *J. Athletic Training*, vol. 37, no. 1, pp. 71–79, Jan. 2002.
[36] B. L. Riemann and S. M. Lephart, "The sensorimotor system, Part II: The role of proprioception in motor control and functional joint stability," *J. Athletic Training*, vol. 37, no. 1, pp. 80–84, Jan. 2002.
[37] T. D. Satterthwaite *et al.*, "An improved framework for confound regression and filtering for control of motion artifact in the preprocessing of resting-state functional connectivity data," *Neuroimage*, vol. 64, pp. 240–256, 2013.
[38] C. Yan *et al.*, "A comprehensive assessment of regional variation in the impact of head micromovements on functional connectomics," *Neuroimage*, vol. 76, pp. 183–201, 2013.
[39] M. Reuter *et al.*, "Head motion during MRI acquisition reduces gray matter volume and thickness estimates," *Neuroimage*, vol. 107, pp. 107–115, 2015.
[40] J. D. Power, K. A. Barnes, A. Z. Snyder, B. L. Schlaggar, and S. E. Petersen, "Spurious but systematic correlations in functional connectivity MRI networks arise from subject motion," *Neuroimage*, vol. 59, no. 3, pp. 2142–2154, 2012.
[41] T. D. Satterthwaite *et al.*, "Impact of in-scanner head motion on multiple measures of functional connectivity: Relevance for studies of neurodevelopment in youth," *Neuroimage*, vol. 60, no. 1, pp. 623–632, 2012.
[42] E. Seto *et al.*, "Quantifying head motion associated with motor tasks used in fMRI," *Neuroimage*, vol. 14, no. 2, pp. 284–297, 2001.
[43] W. Huijbers, K. R. Van Dijk, M. M. Boenniger, R. Stirnberg, and M. M. Breteler, "Less head motion during MRI under task than resting-state conditions," *Neuroimage*, vol. 147, pp. 111–120, 2017.
[44] S. Haller *et al.*, "Head motion parameters in fMRI differ between patients with mild cognitive impairment and Alzheimer disease versus elderly control subjects," *Brain Topogr.*, vol. 27, no. 6, pp. 801–807, 2014.
[45] R. N. Boubela *et al.*, "Beyond noise: Using temporal ICA to extract meaningful information from high-frequency fMRI signal fluctuations during rest," *Front. Hum. Neurosci.*, vol. 7, pp. 1–12, 2013.
[46] J. E. Chen and G. H. Glover, "BOLD fractional contribution to resting-state functional connectivity above 0.1 Hz," *NeuroImage*, vol. 107, pp. 207–218, 2015.